Velocity Determinations for Magnetoacoustic Shock Waves from SOHO/EIT Images

Article *in* Romanian Astronomical Journal · January 2009

1 author:

Adrian Sabin Popescu
Astronomical Institute of Romania

VELOCITY DETERMINATIONS FOR MAGNETOACOUSTIC SHOCK WAVES FROM SOHO/EIT IMAGES

ADRIAN SABIN POPESCU

Astronomical Institute of the Romanian Academy
Str. Cuțitul de Argint 5, 040557 Bucharest, Romania
E-mail: sabinp@aira.astro.ro

Abstract. We use a new multi-wavelength technique applied to the solar corona SOHO/EIT images containing magnetoacoustic waves (EIT waves). In this way we constrain the wave phase velocity. We give, as well, some β-model correlations with height for the vertical extent of the wave. We apply them to the particular EIT wave triggered by the eruptive event from 15 August 2001.

Key words: solar corona – extreme ultraviolet – plasma waves.

1. INTRODUCTION

The method employed in this paper was developed in the IDL computing environment and described by Popescu and Mierla (2008). It is an extremely useful method in determining the solar waves phase velocity. We apply it here to the eruptive event from 15 August 2001 seen by the SOHO/EIT instrument (Delaboudinière et al. 1995). The data are provided by the SOHO/EIT Consortium (to be found on the site `http://umbra.nascom.nasa.gov/eit`). The EIT instrument aboard SOHO observes the Sun in four different wavelengths, namely 171 Å (Fe IX/Fe X; 1.3×10^6 K), 195 Å (Fe XII; 1.6×10^6 K), 284 Å (Fe XV; 2.0×10^6 K) and 304 Å (He II; 8.0×10^4 K), and, consequently, from high chromosphere to mid-corona.

After the description of the method and of its limitations, we will focus on the interpretation of our results, in close correlation with the height related solar features observed into the specified wavelengths. For 195 Å, the only wavelength for which the acquisition rate is of around 12 minutes, we are able to study the temporal evolution of these velocity associated features (CME, EIT wave and horizontal motions). We also show that the EIT wave is a fast magnetoacoustic shock wave whose propagation depends strongly on the solar activity background.

Rom. Astron. J., Vol. **19**, No. 2, p. 000–000, Bucharest, 2009

2. METHODOLOGY

In a simplified vision of the method, at a specific wavelength, two EIT images are subtracted one from the other, to obtain a running differences map of the Sun. This map contains information related to the velocities of the moving solar formations (the displacement over the temporal delay separating the images). Subsequently, we subtract the second EIT image from a third one, having as result another velocity map. Lastly, we subtract the result of the first subtraction from the result of the second one, obtaining an acceleration map (Fig. 1 in Section 3). Requiring that the acceleration map contains only the region in which we observe the EIT wave propagation, and no other parasitic coronal plasma movements, associated to other phenomena, the resulting image has to be cropped. On this cropped image we apply the Fast Fourier Transform (FFT), having as consequence a conversion of the image into a phase space velocity map (Fig. 2 in Section 3). In this image we have to be able to identify individual lines of plasma elements phase velocities. Following the EIT instrument acquisition cadence for a specific wavelength, we repeat the above procedure for all the 15 August 2001 SOHO/EIT images.

Unfortunately, the described method also depends very much on the number of active regions that the EIT wave crosses in its propagation, each one of them introducing unwanted velocity lines into the FFT velocity maps. For the method of processing the cropped image (the same for all the studied images), our ability of seeing the lines of interest, corresponding to:

– the EIT waves;

– the lines of the event triggering the wave (CME, flare, or type II radio burst);

– the ones to be used as etalon (horizontal plasma motions of an origin to be explained later),

constrains us to a small enough number of moving plasma regions. At the same time, the cropped box has to be large enough in order to contain the EIT wave in its movement for a large number of FFT processed images.

3. RESULTS AND DISCUSSION

For a comparative behavior of the EIT waves at different heights in the chromosphere and corona, a good approach is to study them by analyzing the plasma β parameter. It contains the necessary information related to the kinetic and magnetic effects. It has been proved by Gary (2001) that the plasma β-model plays an important role in the solar corona properties and phenomena. The model is particularly useful in dealing with force-free magnetic fields in extrapolation over the whole coronal field range, without assuming $\beta << 1$ in order to overcome the full boundary conditions nonexistence in the two $\beta > 1$ regions. The solutions obtained by Schatten et al. (1969)

neglected the extended influence of the solar wind to low heights, that starts to drag and distort the low solar atmospheric magnetic field (see Altschuler and Newkirk 1969). Also, the outcome of Zhao and Hoeksema (1994) came very close to obtaining a full β coverage of the entire corona, but, unfortunately, they employed artificial cusp surfaces.

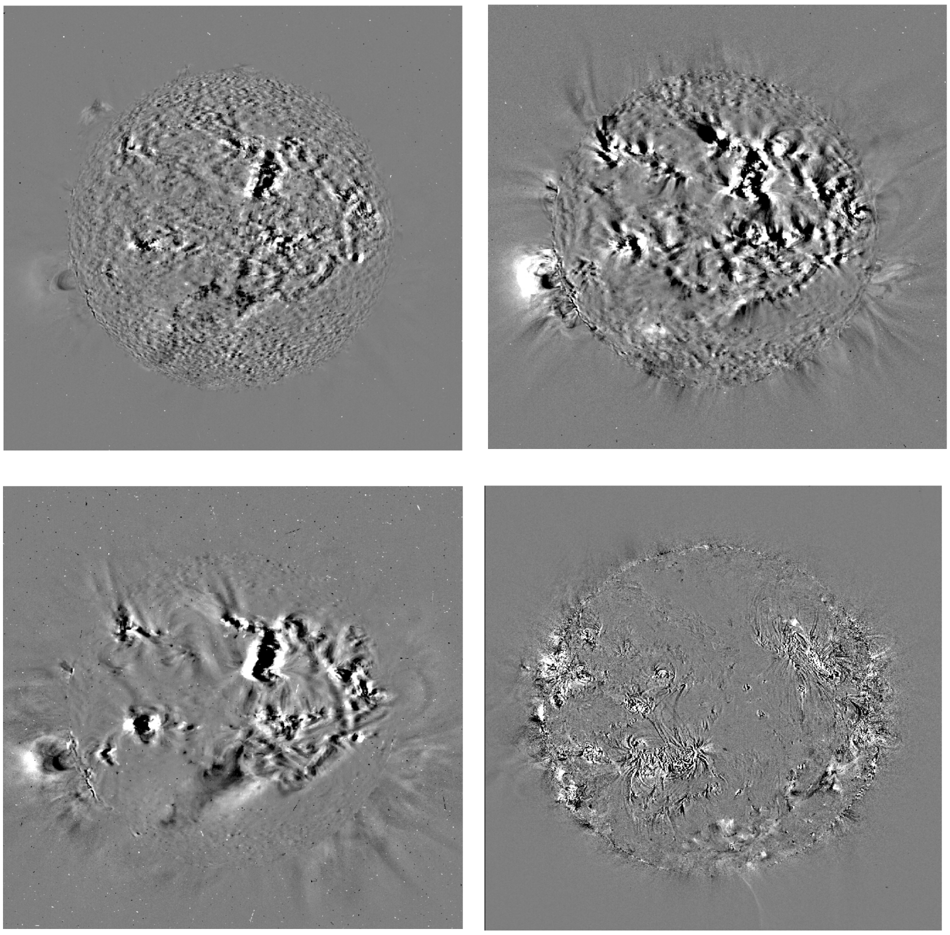

Fig. 1 – Acceleration maps for the 15 August 2001 EIT event in the wavelengths: 304 Å (top left); 171 Å (top right); 195 Å (bottom left); 284 Å (bottom right). In these maps the Sun is vertically flipped from the SOHO/EIT images, with the EIT wave (best visible in 195 Å) at the bottom extremity of the solar acceleration map.

Gary and Alexander (1999) used a set of deformed (by radial stretch) field lines to match the coronal loops, where the observed (SXR/EUV images from SXT, EIT and TRACE) coronal loops were proxies of the upper boundary conditions. They obtained a force-free magnetic field ($\beta < 1$) "sandwiched" between two regions in which $\beta > 1$. Briefly, the model accounts for a more realistic β changes with height, for the unknown boundary conditions on the field and velocities and for the non-force-free effects in the two $\beta > 1$ regions which sandwich the mid-corona. The SOHO/EIT data of Fe IX/Fe X corresponding to a height of 200 Mm has a β range of 0.01–2.0. These values are consistent with this model (see Gary 2001).

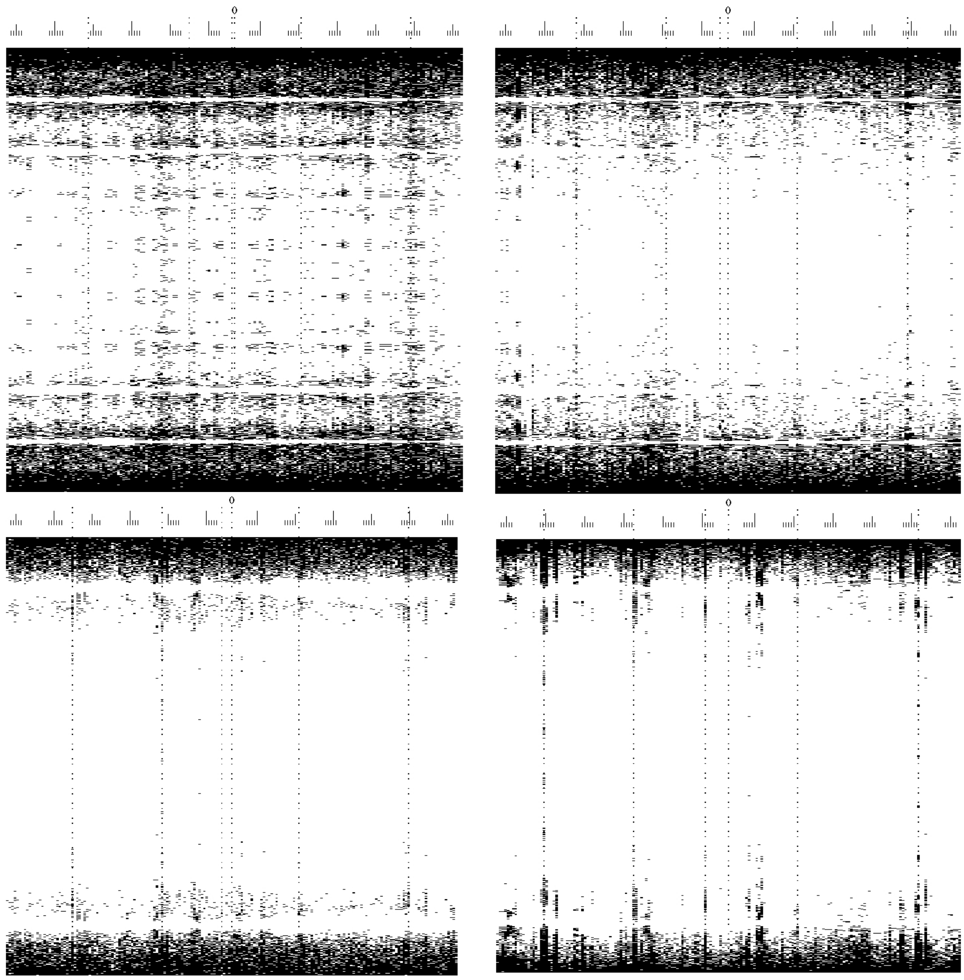

Fig. 2 – Phase-space velocity derived from the acceleration maps (see the text) corresponding to the SOHO/EIT images: 304 Å (top left); 171 Å (top right); 195 Å (bottom left); 284 Å (bottom right). A known velocity (computed by other means) for a phenomenon that can be identified into the EIT images will serve as a scaling rule of all the other velocities present into the images.

An apparent drawback of this β-model is that, asking for simplicity of the representation, it was used only a single pressure model for obtaining the β value. The higher pressures of very hot or non-steady state loops, which represent pressure inside flux tubes, were not used. This made the β values to reach the unity lower than in the corona; see Fig. 3 of Gary (2001) for the plasma β model over an active region. In this way, a lowering in the $\beta = 1$ coronal height will narrow furthermore the "allowed" region of plasma β with $\beta < 1$. This makes that the plasma velocities in the corona at the wavelengths (heights) observed by SOHO/EIT instrument to reflect a more contained movement of plasma, as it can be observed from our FFT velocity maps, too. Within the framework described above, we have compared Gary's (2001) plasma model representation as function of height with our results. It can be observed that, for the high chromosphere 304 Å wavelength, due to a wider β allowance, we will have a greater velocity dispersion in the phase space. From here it follows a larger number of lines in the corresponding FFT maps (see Fig. 2 above) associated to a large number of plasma movements frozen in the field. As the height increases, with the increase of temperature in the mid-corona, from wavelengths 171 Å, to 195 Å, and, finally, 284 Å, we have a decrease in the velocity map lines number, consistent with the narrowing of the β (where $\beta < 1$) allowed region (see Gary 2001), behavior observed also in the associated FFT velocity maps (see Fig. 2).

Except the 304 Å velocity maps, overcrowded with lines, we can observe that all lines identified in the 195 Å maps are still present for the other two EUV wavelengths observed by the EIT instrument.

By comparing the evolution of the same velocity line for different wavelengths, we observe that the velocity of the phenomena giving these lines increases with the height. In the case of the propagating wave, the crest is moving faster than the leading or trailing edge, this causing a steepening of the front portion of the wave and the formation of a steady shock wave in which the dissipative effects equilibrate the convective steepening effects. Into the SOHO/EIT images the dissipative effects can be identified as luminous features on the crest of the two wavefronts. This steepening is consistent with the behavior of a compression wave described by Priest (1987), and even more, with a fast magnetoacoustic wave, the magnetic field before the wavefronts intensifying and being seen as "dimming" regions propagating in front of the shocks.

We must specify the fact that the lines contained between the EIT and the horizontal inter-shocks plasma motions (on both sides of the zero point) represent the signature of the CME projection in the image plane. Following the temporal evolution at 195 Å, we observed a shift of these two lines (in contrast with the EIT associated lines, that kept their position) toward the zero point, the CME associated phase velocity decreasing with time.

Perusing Fig. 2, we observe that the velocity increases radically with height for the lines to the left of zero, while the ones to its right present just a slight increase. The reason for this behavior will be found by returning to the EIT images where we observe that one side of the wavefront is bouncing into the active region 09775, being decelerated. With the height increase, the magnetic field lines over this active region cover a wider region in the corona, rotating, as the fast shock passes, away from the shock normal (Priest 1987) and forcing the EIT and CME shock waves to adopt a larger tilt angle relative to the solar surface. On the other side, away from the active region, the EIT and CME propagation do not meet any resistance from the solar background. This difference between the two wavefronts gives rise to an excess of magnetic pressure that must relax by plasma movement from high to low pressure regions. This movement can be seen in the EIT images as arcades uniting the two EIT wavefronts, and moving away from the mentioned active region.

As it is known, in EUV, in the transition zone between the chromosphere and corona (Athay et al. 1980; Malherbe and Priest 1983), the horizontal flows in the proximity of a prominence are usually between 5 and 20 km/s. For the 15 August 2001 EIT wave, in the Fig. 2 maps, the velocity line close by the central zero point (the zero velocity) represents the velocity of the inter-wavefronts flows described above. In the wavelength 284 Å maps, taking this phase velocity as being 20 km/s, the EIT wavefronts phase velocity (first and last lines in the map) will be of about 160 km/s. Scaling the velocity in all the maps with the velocity of the inter-wavefronts flow for 284 Å, considered to be 20 km/s, we obtain, as function of EUV wavelength, the values from Table 1. Translating the wavelength values into the corresponding plasma temperature values, we can actually follow the extent of the waves into the solar atmosphere as represented in Fig. 3. A more precise determination of the two EIT wavefronts velocity will require a more precise determination of the etalon horizontal motion.

Table 1

Plasma velocities from Fig. 2, FFT maps as function of wavelength, scaled with the 284 Å inter-wavefronts plasma flow at 20 km/s.

	Wavelength [Å]	304	171	195	284
	Temperature [K]	8×10^4	1.3×10^6	1.6×10^6	2×10^6
Velocity [km/s]	Line 1	–128.056	–130.311	–141.247	–158.895
	Line 2	–39.73	–53.148	–61.719	–81.739
	Line 3	–2.3	–6.845	–8.841	–20
	Line 4	58.281	59.431	59.451	59.451
	Line 5	154.341	154.341	156.622	163.472

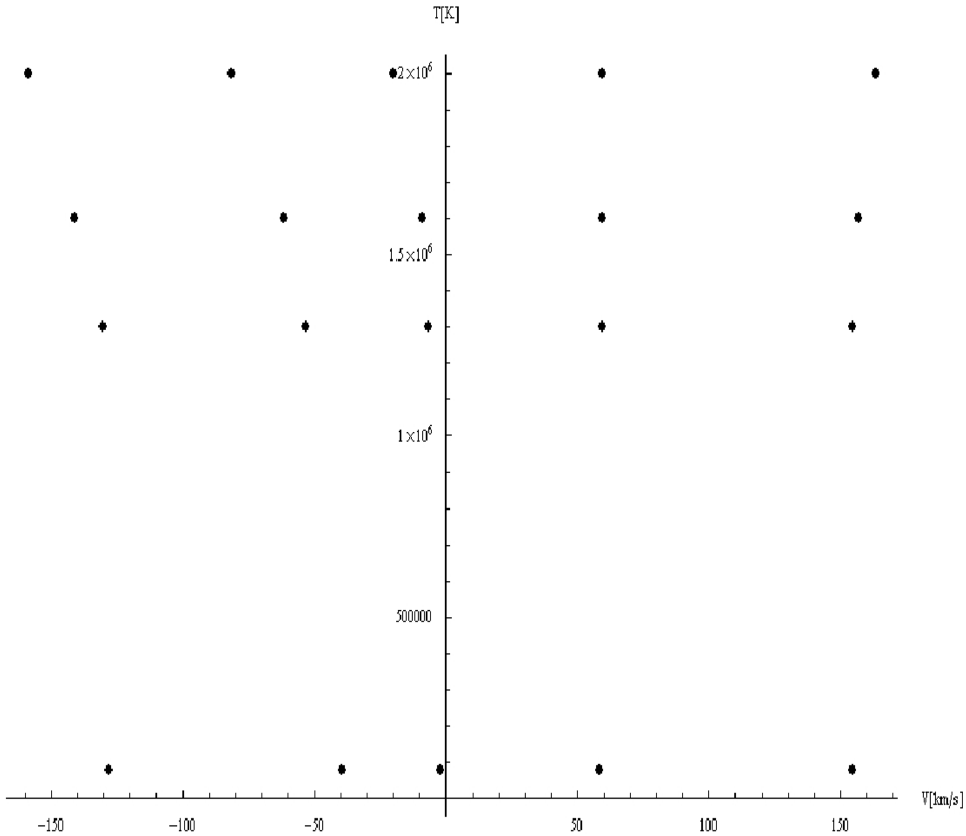

Fig. 3 – Extent of the magnetoacoustic shock waves into the solar atmosphere as function of temperature. The scaling is done in 284 Å, considering that plasma velocity of the inter-wavefronts flow is 20 km/s.

Acknowledgments. The author duly acknowledges the valuable suggestions and advices of Drs José Luis Ballester and Cristiana Dumitrache, intended to improve the presentation of the paper. The contribution of the Editorial Board of the *Romanian Astronomical Journal* is also acknowledged. I would also like to thank the SOHO/EIT consortium for providing me with the data and the calibration software libraries. SOHO is a project of international cooperation between ESA and NASA.

REFERENCES

Altschuler, M. D., Newkirk, G.: 1969, *Solar Phys.*, **9**, 131.

Athay, R .G., White, O. R., Lites, B. W., Bruner, E. C.: 1980, *Solar Phys.*, **66**, 357.

Delaboudinière, J.-P., Artzner, G. E., Brunaud, J., Gabriel, A. H., Hochedez, J. F., Millier, F., Song. X. Y., Au, B., Dere, K. P., Howard, R. A., Kreplin, R., Michels, D. J., Moses, J. D., Defise, J. M., Jamar, C., Rochus, P., Chauvineau, J. P., Marioge, J. P., Catura, R. C., Lemen, J. R., Shing, L., Stern, R. A., Gurman, J. B., Neupert, W. M., Maucherat, A., Clette, F., Cugnon, P., van Dessel, E. L.: 1995, *Solar Phys.*, **162**, 291.

Gary, G. A.: 2001, *Solar Phys.*, **203**, 71.
Gary, G. A., Alexander, D.: 1999, *Solar Phys.*, **186**, 123.
Priest, E. R.: 1987, *Solar Magneto-Hydrodynamics*, D. Reidel Publ. Co., Dordrecht, Holland.
Malherbe, J.H., Priest, E.R.: 1983, *Astron. Astrophys.*, **123**, 80.
Popescu, A. S., Mierla, M.: 2008, in V. Mioc, C. Dumitrache, N. A. Popescu (eds), *Exploring the Solar System and the Universe*, Amer. Inst. Phys. Conf. Proc. Series, Vol. **1043**, Melville, NY, p. 309.
Schatten, K. H., Wilcox, J. M., Ness, N. F.: 1969, *Solar Phys.*, **6**, 442.
Zhao, X., Hoeksema, J. T.: 1994, *Solar Phys.*, **151**, 91.

Received on 27 June 2009